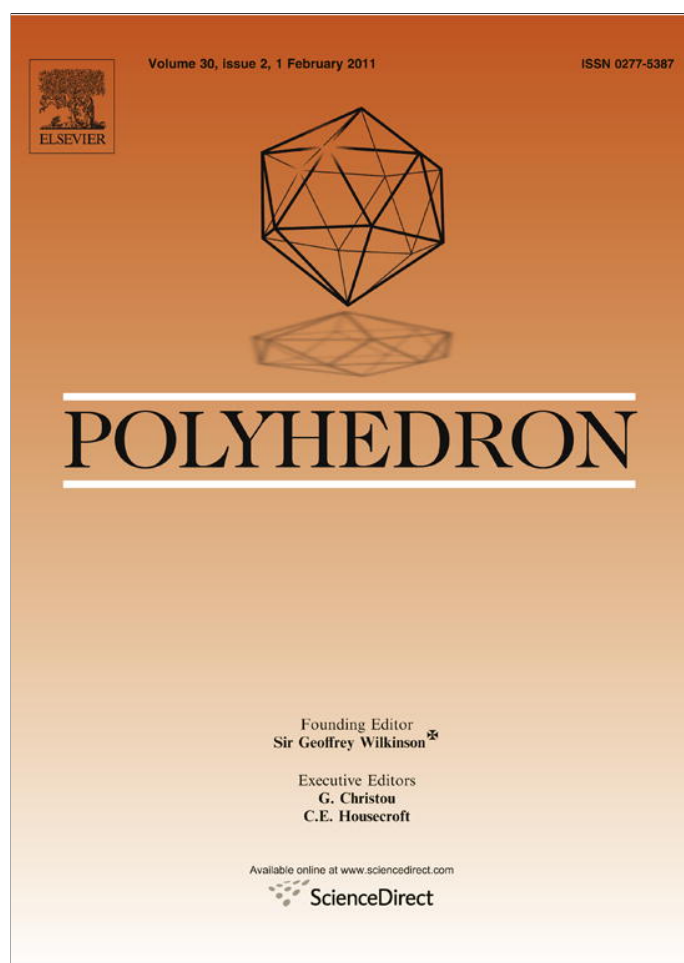


Provided for non-commercial research and education use.  
Not for reproduction, distribution or commercial use.



This article appeared in a journal published by Elsevier. The attached copy is furnished to the author for internal non-commercial research and education use, including for instruction at the authors institution and sharing with colleagues.

Other uses, including reproduction and distribution, or selling or licensing copies, or posting to personal, institutional or third party websites are prohibited.

In most cases authors are permitted to post their version of the article (e.g. in Word or Tex form) to their personal website or institutional repository. Authors requiring further information regarding Elsevier's archiving and manuscript policies are encouraged to visit:

<http://www.elsevier.com/copyright>



Contents lists available at ScienceDirect

Polyhedron

journal homepage: [www.elsevier.com/locate/poly](http://www.elsevier.com/locate/poly)

# Low-dimensional compounds containing cyanido groups. XXI. Crystal structure, spectroscopic, thermal and magnetic properties of two polymorphous modifications of $[\text{Cu}(\text{men})_2\text{Pt}(\text{CN})_4]_n$ complex ( $\text{men} = N$ -methyl-1,2-diaminoethane)

Martin Vavra<sup>a,\*</sup>, Ivan Potočňák<sup>a</sup>, Erik Čížmár<sup>b</sup>, Marcela Kajňaková<sup>b</sup>, Michal Dušek<sup>c</sup>, Harry Schmidt<sup>d</sup>, Mykhaylo Ozerov<sup>e</sup>, Sergej A. Zvyagin<sup>e</sup>, L'ubor Dlháč<sup>f</sup>, Roman Boča<sup>g</sup>

<sup>a</sup> Department of Inorganic Chemistry, Institute of Chemistry, P.J. Šafárik University, Moyzesova 11, SK-04154 Košice, Slovakia

<sup>b</sup> Centre of Low Temperature Physics, Faculty of Science, P.J. Šafárik University and IEP SAS, Park Angelinum 9, SK-04154 Košice, Slovakia

<sup>c</sup> Institute of Physics, Na Slovance 2, CZ-182 21 Praha 8, Czech Republic

<sup>d</sup> Institute of Inorganic Chemistry, Martin-Luther-University, Halle-Wittenberg, Kurt-Mothes-Str. 2, D-06120 Halle, Germany

<sup>e</sup> Dresden High Magnetic Field Laboratory (HLD), Research Center Dresden-Rossendorf (FZD), 01314 Dresden, Germany

<sup>f</sup> Institute of Inorganic Chemistry, Technology and Materials, FCHPT, Slovak University of Technology, Radlinského 9, SK-81237 Bratislava, Slovakia

<sup>g</sup> Department of Chemistry (FPV), University of SS Cyril and Methodius, SK-91701 Trnava, Slovakia

## ARTICLE INFO

### Article history:

Received 14 July 2010

Accepted 19 October 2010

Available online 26 October 2010

### Keywords:

1D crystal structure

Polymorphous modifications

$N$ -methyl-1,2-diaminoethane

Tetracyanidoplatinate(II)

Infrared spectroscopy

Spectral–structural correlations

Antiferromagnetic exchange

## ABSTRACT

Violet (**1**) and blue (**2**) polymorphous modifications of  $[\text{Cu}(\text{men})_2\text{Pt}(\text{CN})_4]_n$  ( $\text{men} = N$ -methyl-1,2-diaminoethane) have been prepared and investigated by IR and UV–vis spectroscopy, thermal analysis, measurement of magnetic data and X-ray structural analysis. Both modifications are formed by similar but differently packed zigzag chains, which consist of  $[\text{Cu}(\text{men})_2]^{2+}$  moieties bridged by two *trans* arranged cyanido groups of  $[\text{Pt}(\text{CN})_4]^{2-}$  units. The Cu(II) atoms in both structures are hexacoordinated by four nitrogen atoms in the equatorial plane from two molecules of bidentate *men* ligands with the average Cu–N(Me) and Cu–N(H<sub>2</sub>) bond lengths of 2.046(8) and 2.008(8) Å, respectively, and by two nitrogen atoms from bridging cyanido groups in the axial positions at average distance of 2.50(7) Å. Broad nearly symmetric bands observed in the UV–vis spectra of **1** and **2** of  ${}^2B_{1g} \rightarrow {}^2E_g$  transitions are consistent with a deformed octahedral coordination of the  $\text{CuN}_6$  chromophoric groups. One and two  $\nu(\text{C}\equiv\text{N})$  absorption bands observed in the IR spectra of **1** and **2**, respectively, are in agreement with different local symmetries of  $[\text{Pt}(\text{CN})_4]^{2-}$  units and different Cu–N(cyanido) bond lengths in these polymorphs and are subject of discussion on the spectral–structural correlations in 1D compounds. The complexes are stable up to 238 °C when their two-stage thermal decompositions start and ending up with a mixture of CuO and metallic Pt as the most probable final thermal decomposition products. The temperature dependence of the magnetic susceptibility suggests the presence of a weak antiferromagnetic exchange coupling between Cu(II) atoms in **1**,  $J/hc = -0.17 \text{ cm}^{-1}$  and in **2**,  $J/hc = -1.3 \text{ cm}^{-1}$ .

© 2010 Elsevier Ltd. All rights reserved.

## 1. Introduction

The cyanide moiety  $\text{C}\equiv\text{N}$  can act as a terminal or bridging ligand. In most compounds with bridging cyanide, polymeric one- (1D), two- (2D) or three-dimensional (3D) networks are observed in the solid state. As has been reviewed, interest has been drawn to cyanide-containing systems such as the Prussian blue compounds [1], the Hofmann clathrates [2], or low-dimensional compounds [3], largely because of their potentially useful physical or chemical properties. However, in spite of all the research done in this field, it is still difficult to predict the structure or even the dimensionality of a new compound of this class [4].

In our previous studies on the role of hydrogen bonds as possible exchange paths for magnetic interactions in low-dimensional compounds we have prepared and characterized compounds of general formula  $[\text{Cu}(L)_2\text{Pt}(\text{CN})_4]_n$ , where  $L$  are bidentate  $N$ -donor ligands: 1,2-diaminoethane (*en*), its  $N,N'$ - (*bmen*) and  $N,N$ -dimethyl (*dmen*) derivatives, and 2,2'-bipyridine (*bpy*). Crystal structure analysis has revealed that their structures are formed by 1D zigzag chains stabilized by hydrogen bonds [5–7]. Within this studies we have also investigated a correlation between the number of different cyanido groups in the structures and the number of  $\nu(\text{C}\equiv\text{N})$  vibrations in the IR spectra to predict the dimensionality of the prepared compounds, as well as correlation between the Cu–N(cyanido) bond lengths and the wavenumbers of  $\nu(\text{C}\equiv\text{N})$  vibrations. We have found that the longer Cu–N(cyanido) bond lengths, the lower wavenumbers of  $\nu(\text{C}\equiv\text{N})$  vibrations, sometimes even

\* Corresponding author. Tel.: +421 55 234 2346; fax: +421 55 62 221 24.

E-mail address: [martin.vavra@upjs.sk](mailto:martin.vavra@upjs.sk) (M. Vavra).

leading to the smaller number of observed  $\nu(\text{C}\equiv\text{N})$  vibrations than expected. To confirm these observations we tried to prepare other 1D compounds of  $[\text{Cu}(L)_2\text{Pt}(\text{CN})_4]_n$  composition with bidentate *N*-donor ligands 1,10-phenanthroline, 1,2- and 1,3-diaminopropane, nevertheless the corresponding syntheses resulted in products of unexpected compositions with oligonuclear particles or 2D structures [8,9]. Therefore we have decided to prepare the desired 1D compound using another derivative of *en*, *N*-methyl-1,2-diaminoethane (*men*). As a result of our efforts, two polymorphous modifications of  $[\text{Cu}(\text{men})_2\text{Pt}(\text{CN})_4]_n$  were prepared. In this paper we present their preparation, crystal structures, spectral, thermal and magnetic properties and we discuss the above mentioned spectral–structural correlations as well.

## 2. Experimental

### 2.1. Materials

Copper chloride dihydrate ( $\text{CuCl}_2 \cdot 2\text{H}_2\text{O}$ ), copper sulfate pentahydrate ( $\text{CuSO}_4 \cdot 5\text{H}_2\text{O}$ ) and *men* ( $\text{C}_3\text{H}_{10}\text{N}_2$ ) were of Aldrich quality and used as received.  $\text{K}_2[\text{Pt}(\text{CN})_4] \cdot 3\text{H}_2\text{O}$  was prepared according to the literature [10].

### 2.2. Physical measurements

Elemental analyses for C, H and N were carried out using a LECO CHNS-932. IR spectra were recorded on an Avatar 330 FT-IR spectrometer by the method of KBr pellets in the range from 4000 to  $400\text{ cm}^{-1}$ . UV–vis spectra in Nujol suspensions were measured with a Specord 250 in the range from 300 to 1100 nm. The thermal investigations were performed using NETZSCH STA 409 PC/PG thermal analyzer under air conditions with a heating rate of  $9\text{ }^\circ\text{C}/\text{min}$  to  $900\text{ }^\circ\text{C}$ . EPR data were collected at low temperatures in an X-band Bruker ELEXSYS E500 spectrometer. Measurement of the magnetic susceptibility was carried out using a commercial SQUID magnetometer (Quantum Design) in the temperature range between 2 and 300 K. The correction for an underlying diamagnetism, estimated using Pascal's constants [11] ( $\chi_{\text{DIA}} = -2.75 \times 10^{-9}\text{ m}^3\text{ mol}^{-1}$ ), was applied.

### 2.3. Synthesis and characterization

$[\text{Cu}(\text{men})_2\text{Pt}(\text{CN})_4]_n$  violet (**1**) and blue (**2**). Into stirring water–methanol solution (1:1) of  $\text{CuCl}_2$  (0.085 g  $\text{CuCl}_2 \cdot 2\text{H}_2\text{O}$ , 0.5 mmol), *men* (0.18 ml, 2 mmol) was added in one portion and after 30 min of stirring, aqueous solution of  $\text{K}_2[\text{Pt}(\text{CN})_4]$  (0.216 g  $\text{K}_2[\text{Pt}(\text{CN})_4] \cdot 3\text{H}_2\text{O}$ , 0.5 mmol) (1.4:1 molar ratio) was added in one portion, too. After a few days, violet crystals of **1**, with a quality not suitable for X-ray single crystal analysis, were filtrated off and dried on air and their IR spectrum was measured. Yield 0.197 g (77%). The crystals suitable for X-ray analysis have been prepared by a different procedure using  $\text{CuSO}_4 \cdot 5\text{H}_2\text{O}$  (0.125 g, 0.5 mmol); *men* (0.09 ml, 1.0 mmol) and  $\text{K}_2[\text{Pt}(\text{CN})_4] \cdot 3\text{H}_2\text{O}$  (0.216 g, 0.5 mmol) (1.2:1) dissolved in 6 ml of water under hydrothermal conditions in autoclave in a programmable heater at  $100\text{ }^\circ\text{C}$  for 80 h. After cooling down to the room temperature during 13 h, blue crystals of **2** were isolated from a blue powder of **2**. In order to prepare violet crystals of **1** suitable for X-ray analysis we used hydrothermal synthesis once again using the same conditions, but with an excess of *men* (0.14 ml, 1.5 mmol) (1.3:1). After cooling down to the room temperature, violet crystals of **1** were filtrated off and dried on air. The IR spectra of violet crystals of **1** prepared by above mentioned different ways were identical.

Complex **1**: IR (4000–400  $\text{cm}^{-1}$ , KBr pellets):  $\nu(\text{N}-\text{H}) = 3316\text{ vs}$ , 3259 vs, 3160 m;  $\nu(\text{C}-\text{H}) = 2998\text{ w}$ , 2982 m, 2970 m, 2957 m, 2907

w, 2882 w;  $\nu(\text{C}\equiv\text{N}) = 2130\text{ vs}$ ;  $\delta(\text{NH}_2) = 1588\text{ s}$ ;  $\delta(\text{CH}_2)$  and  $\delta(\text{CH}_3) = 1471\text{ s}$ , 1450 m, 1435 w, 1416 w;  $\tau(\text{CH}_2) = 1281\text{ m}$ ;  $\tau(\text{NH}_2) = 1066\text{ s}$ ;  $\nu(\text{C}-\text{N}) = 1019\text{ m}$ ;  $\nu(\text{C}-\text{C}) = 957\text{ s}$ ;  $\nu(\text{Pt}-\text{C}) = 497\text{ m}$ , 452 w, 406 m. UV–vis (solid state):  $\lambda_{\text{max}} = 545\text{ nm}$  ( ${}^2\text{B}_{1g} \rightarrow {}^2\text{E}_g$  transition). Elemental Anal. Calc. for  $\text{C}_{10}\text{H}_{20}\text{CuN}_8\text{Pt}$ : C, 23.51; H, 3.95; N, 21.93. Found: C, 23.63; H, 4.45; N, 21.46%.

Complex **2**: IR: (4000–400  $\text{cm}^{-1}$ , KBr pellets):  $\nu(\text{N}-\text{H}) = 3279\text{ s}$ , 3240 m, 3163 m;  $\nu(\text{C}-\text{H}) = 2976\text{ w}$ , 2933 m, 2916 m, 2881 w;  $\nu(\text{C}\equiv\text{N}) = 2129\text{ vs}$ , 2119 s;  $\delta(\text{NH}_2) = 1603\text{ m}$ ;  $\delta(\text{CH}_2)$  and  $\delta(\text{CH}_3) = 1477\text{ w}$ , 1448 m, 1439 m;  $\tau(\text{CH}_2) = 1279\text{ w}$ ;  $\tau(\text{NH}_2) = 1093\text{ s}$ ;  $\nu(\text{C}-\text{N}) = 1049\text{ m}$ , 1030 m;  $\nu(\text{C}-\text{C}) = 970\text{ s}$ ;  $\nu(\text{Pt}-\text{C}) = 455\text{ w}$ , 415 m. UV–vis (solid state):  $\lambda_{\text{max}} = 580\text{ nm}$  ( ${}^2\text{B}_{1g} \rightarrow {}^2\text{E}_g$  transition). Elemental Anal. Calc. for  $\text{C}_{10}\text{H}_{20}\text{CuN}_8\text{Pt}$ : C, 23.51; H, 3.95; N, 21.93. Found: C, 23.27; H, 3.87; N, 21.76%.

### 2.4. X-ray data collection and structure refinement

A summary of crystal and structure refinement data for **1** and **2** is presented in Table 1. Both crystal structures were determined using an Oxford Diffraction Xcalibur2 diffractometer equipped with a Sapphire2 CCD detector. CrysAlis CCD was used for data collection while CrysAlis RED was used for the cell refinement, data reduction and absorption correction [12]. The structure of **1** was solved by the direct method with SHELXS97 and subsequent Fourier syntheses using SHELXL97 [13] while the structure of **2** was solved by JANA2006 [14] first and then redetermined using SHELXL97. The anisotropic displacement parameters were refined for all non-H atoms. The H atoms were placed in calculated positions and refined riding on their parent C or N atoms with C–H distances of 0.97 and 0.96 Å for methylene and methyl H atoms, respectively, and with N–H distances of 0.90 Å and 0.91 Å for primary and secondary amino H atoms, respectively, and  $U_{\text{iso}}(\text{H}) = 1.2U_{\text{eq}}(\text{C or N})$ . An analysis of bond distances and angles was performed using SHELXL97 [13], DIAMOND [15] was used for molecular graphics.

## 3. Results and discussions

### 3.1. Preparation of the title complexes

The title complex **1** has been prepared in a relatively simple way within our studies on the role of hydrogen bonds as possible exchange paths for magnetic interactions in low-dimensional compounds and within our studies on the effect of Cu–N(cyanido) bond length on the wavenumber of corresponding  $\nu(\text{C}\equiv\text{N})$  vibration. To prepare the desired complex, we have used the same procedure and the same Cu(II), *men* and  $[\text{Pt}(\text{CN})_4]^{2-}$  molar ratios as were used in the preparation of the previous chain-like  $[\text{Cu}(L)_2\text{Pt}(\text{CN})_4]_n$  complexes ( $L = \text{en}$ , *dmen*, *bmen* and *bpy*) [5–7]. Nevertheless, prepared violet crystals of **1** were of a poor quality and therefore hydrothermal reaction conditions were used. During our successful attempts to prepare crystals of **1** suitable for X-ray analysis, blue crystals of **2** were accidentally prepared, too. Although the IR and UV–vis spectra of **1** and **2** were different, the results of the elemental analysis of both complexes are in good agreement with an expected  $[\text{Cu}(\text{men})_2\text{Pt}(\text{CN})_4]_n$  composition, thus indicating two polymorphous modifications of the same compound. This was definitely confirmed by the X-ray analysis which revealed that compounds **1** and **2** have similar chain-like structure with the  $[\text{Cu}(\text{men})_2\text{Pt}(\text{CN})_4]_n$  formula but their symmetry differs.

### 3.2. X-ray crystallography

X-ray analysis has revealed that crystal structures of **1** and **2** are similar and are formed by 1D zigzag chains which consist of  $[\text{Cu}(\text{men})_2]^{2+}$  moieties bridged by two *trans* arranged cyanido groups

**Table 1**  
Crystal data and structure refinement of **1** and **2**.

	<b>1</b>	<b>2</b>
Empirical formula	C <sub>10</sub> H <sub>20</sub> CuN <sub>8</sub> Pt	C <sub>10</sub> H <sub>20</sub> CuN <sub>8</sub> Pt
Formula weight	510.97	510.97
T (K)	293(2)	293(2)
λ (Å)	0.71073	0.71073
Crystal system	triclinic	tetragonal
Space group	P $\bar{1}$	P4 <sub>2</sub> /m
Unit cell dimensions		
a (Å)	7.3529(3)	10.18372(14)
b (Å)	7.4376(3)	10.18372(14)
c (Å)	7.7496(3)	7.55607(19)
α (°)	101.207(4)	
β (°)	97.866(4)	
γ (°)	102.927(4)	
V (Å <sup>3</sup> )	397.92(3)	783.63(2)
Z; D <sub>calc</sub>	1; 2.132 g cm <sup>-3</sup>	2; 2.165 g cm <sup>-3</sup>
Absorption coefficient (mm <sup>-1</sup> )	10.119	10.276
F(0 0 0)	243	486
Crystal shape, color	plate, violet	prism, blue
Crystal size (mm <sup>3</sup> )	0.27 × 0.19 × 0.08	0.28 × 0.10 × 0.07
θ range for data collection (°)	2.73–26.58	2.83–27.00
Index ranges	−9 ≤ h ≤ 9, −9 ≤ k ≤ 9, −9 ≤ l ≤ 9	−12 ≤ h ≤ 13, −13 ≤ k ≤ 13, −9 ≤ l ≤ 9
Absorption correction	analytical [16]	analytical [16]
Max. and min. transmission	0.553 and 0.174	0.598 and 0.188
Reflections collected/unique (R <sub>int</sub> )	6953/1667 (0.0311)	15591/918 (0.0487)
Completeness to θ <sub>max</sub> (%)	100.0	99.8
Refinement method	full-matrix least-squares on F <sup>2</sup>	full-matrix least-squares on F <sup>2</sup>
Data/restraints/parameters	1667/0/95	918/0/79
Goodness-of-fit (GOF) on F <sup>2</sup>	1.007	0.953
Final R factors [I > 2σ(I)]	R <sub>1</sub> = 0.0148, wR <sub>2</sub> = 0.0341	R <sub>1</sub> = 0.0130, wR <sub>2</sub> = 0.0288
R factors (all data)	R <sub>1</sub> = 0.0148, wR <sub>2</sub> = 0.0341	R <sub>1</sub> = 0.0220, wR <sub>2</sub> = 0.0302
Largest difference in peak and hole (e Å <sup>-3</sup> )	0.400 and −0.619	1.132 and −0.309

of [Pt(CN)<sub>4</sub>]<sup>2-</sup> units. A DIAMOND view with the atomic numbering scheme of these compounds is depicted in Figs. 1 and 2, respectively, and selected bond lengths and bond angles for both compounds are given in Table 2. These complexes represent structural analogs of the [Cu(L)<sub>2</sub>M(CN)<sub>4</sub>]<sub>n</sub> complexes mentioned in Section 1. The Cu(II) atoms in both structures are six-coordinate, complexed with the four nitrogen atoms of two *men* ligands in the equatorial planes and two nitrogen atoms from bridging cyano groups in the axial positions.

The Cu–N bond distances in the equatorial planes of both complexes are not of the same length and the effect of steric repulsion of methyl groups bonded to N3 atoms is clear; whereas the average value of Cu1–N3(Me) bonds is 2.046(8) Å, the average value of Cu1–N4(H<sub>2</sub>) bonds is only 2.008(8) Å. If we compare these values with the respective values found in other [Cu(L)<sub>2</sub>Pt(CN)<sub>4</sub>]<sub>n</sub> complexes we can see that for L = *en* [5], where only Cu–N(H<sub>2</sub>) bonds

are present (2.022(7) Å on average), the Cu1–N3(Me) and Cu1–N4(H<sub>2</sub>) bonds in **1** and **2** are about 0.02 Å longer and shorter, respectively. For L = *bmén* [6], where only Cu–N(Me) bonds are present (2.043(18) Å on average), these bonds are of the same length as the Cu1–N3(Me) bonds in **1** and **2**. Finally, the effect of bulky methyl groups on the Cu–N bond lengths is remarkable for L = *dmén* [5], where both Cu–N(Me<sub>2</sub>) and Cu–N(H<sub>2</sub>) bonds are present (2.115(4) and 1.984(4) Å, respectively). Similar trends in Cu–N bond lengths have been observed in other [Cu(L)<sub>2</sub>M(CN)<sub>4</sub>]<sub>n</sub> complexes containing a bulky group substituting one amino hydrogen atom; e.g. [Cu(*eten*)<sub>2</sub>M(CN)<sub>4</sub>]<sub>n</sub> (*eten* = N-ethyl-1,2-diaminoethane; M = Ni, Pd and Pt) with Cu–N(Et) = 2.056(2), 2.050(2) and 2.054(2) Å, respectively, and Cu–N(H<sub>2</sub>) = 2.008(2), 2.007(2) and 2.010(2) Å, respectively [17,18], [Cu(*hydeten*)<sub>2</sub>Pt(CN)<sub>4</sub>]<sub>n</sub> (*hydeten* = N-(2-hydroxyethyl)-1,2-diaminoethane) with Cu–N(EtOH) = 2.070(4) Å and Cu–N(H<sub>2</sub>) = 2.029(4) Å [19] or in

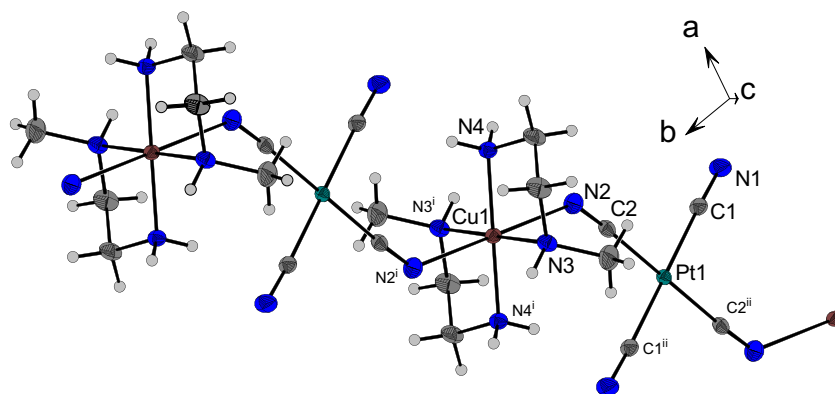


**Fig. 1.** Structure of **1** with displacement ellipsoids (25% probability) and labeling of selected atoms. Symmetry operations: (i) 1 – x, 1 – y, –1 – z and (ii) –x, –y, –2 – z.

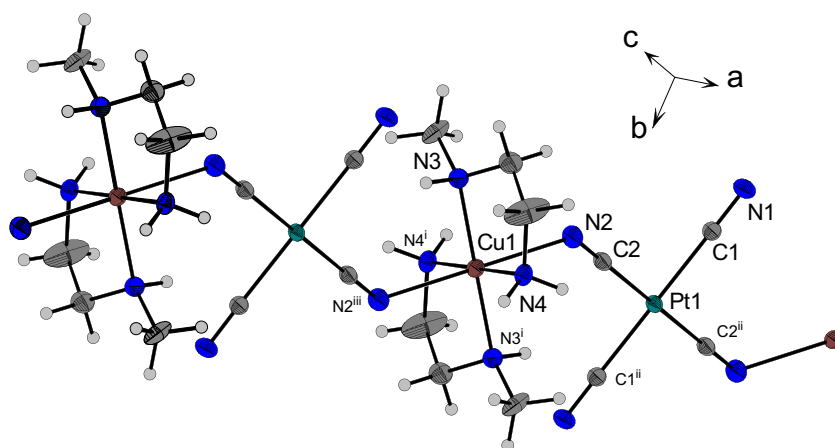


**Fig. 2.** Structure of **2** with displacement ellipsoids (25% probability) and labeling of selected atoms. Symmetry operations: (i)  $-x, 1 - y, -z$ ; (ii)  $1 - x, 1 - y, z$ ; and (iii)  $-x, 1 - y, z$ .

**Table 2**  
Selected bond lengths (Å) and bond angles ( $^{\circ}$ ) of **1** and **2**.

	<b>1</b>	<b>2</b>
Cu1–N2	2.552(3)	2.450(3)
Cu1–N3	2.040(2)	2.051(4)
Cu1–N4	2.003(2)	2.013(4)
Pt1–C1	1.987(3)	1.986(4)
Pt1–C2	1.981(3)	1.977(4)
C1–N1	1.143(4)	1.146(5)
C2–N2	1.146(4)	1.150(5)
C1–Pt1–C2	92.09(11)	88.23(14)
Cu–N2–C2	133.6(2)	131.7(3)
N1–C1–Pt1	176.8(3)	179.0(3)
N2–C2–Pt1	175.6(3)	179.7(3)
N3–Cu1–N2	96.07(10)	91.79(14)
N4–Cu1–N2	85.41(9)	88.33(13)
N4–Cu1–N3	85.61(10)	84.18(18)

analogous  $[\text{Cu}(\text{men})_2\text{Ni}(\text{CN})_4]_n$  complex [20] ( $\text{Cu}-\text{N}(\text{Me}) = 2.037(3)$  and  $\text{Cu}-\text{N}(\text{H}_2) = 1.996(2)$  Å) where these distances are slightly shorter than in **1** and **2**. The Cu–men metalocycles in both coordination polyhedra are in a  $\delta\lambda$  conformation, exhibiting usual values of bond distances and angles within the men molecules.

The axial positions of the distorted octahedral coordination sphere are occupied by the N2 atoms of the bridging cyanido groups and their symmetrically related partners at significantly longer Cu1–N2 distances of 2.552(3) and 2.450(3) Å for **1** and **2**, respectively, due to Jahn–Teller effect which is characteristic for  $d^9$  systems. The Cu1–N2 bonds are tilted from the normals to the CuN4 equatorial planes by 7.93° and 2.60° for **1** and **2**, respectively, forming slightly distorted and tetragonally elongated 4 + 2 octahedral geometries. The corresponding tetragonality  $T$  factors [21] for **1** and **2** are 0.792 and 0.829, respectively.

Square planar  $[\text{Pt}(\text{CN})_4]^{2-}$  moieties, as parts of the zigzag chains, connect Cu(II) atoms by two *trans*-arranged symmetrically related bridging cyanido groups forming thus a 2,2-*TT* chain [3]. Despite the different character of the cyanido groups the average Pt–C and C≡N bond distances as well as Pt–C≡N angles for bridging and terminal cyanido groups in **1** and **2** are very similar and in expected ranges (Table 2). On the other hand, the cyanido groups coordinate to the copper(II) atoms in a significantly bent way as evidenced from the Cu1–N2≡C2 angles of 133.6(2)° and 131.7(3)° for **1** and **2**, respectively. Nevertheless, such values are not unusual and indicate a contribution of the ionic character to the Cu–N bond [5,6,8,17,22–24].

Although the structures of **1** and **2** are formed by very similar zigzag chains, still there are some differences between them con-

sisting in different bond parameters, in different arrangement of methyl groups of men ligands, in different packing of the chains and in different hydrogen bonds (HBs). The most remarkable differences in bond parameters are the Cu1–N2 bonds and the Cu1–N2≡C2 angles, mentioned above, as well as other angles given in the Table 2. Different arrangement of methyl groups of men ligands in **1** and **2** can be recognized in Figs. 1 and 2, respectively, and is evidenced by different values of C–C–N3–Me torsion angles within men molecules in **1** and **2**, which are 89.7 and 179.9°, respectively. Thus, the methyl groups are coordinated to the planes of Cu–men metalocycles in **1** and **2** in nearly perpendicular and parallel fashions, respectively. Moreover, while all atoms of the men ligand in **1** are fully occupied (their site occupation factors, SOFs, are equal to 1), the men ligands in **2** are disordered over two positions with SOFs equal to 0.5. Disordered men ligands in **2** are shown in Fig. 3. The most striking difference in the structures of **1** and **2** is a different packing of the chains. Whereas all chains in **1** run along the [1 1 1] direction being thus mutually parallel (Fig. 4), the chains in **2** are extended along both the *a* and *b* axes. Thus two sets of parallel chains which are perpendicularly crossed, exist in **2** (Fig. 5). Due to the different packing of the chains, both structures are stabilized by different N–H...N HBs systems which involve nitrogen atoms of terminal cyanido and of amino groups as acceptors and donors, respectively, and which connect individual chains into 2D sheets (Fig. 6, Table 3) and 3D network (Fig. 7, Table 4), respectively. The HBs system in **1** is formed by one intrachain HB mediated by N4–H4B...N1<sup>ii</sup> atoms and by two interchain HBs mediated by N4–H4A...N1<sup>i</sup> and N3–H3...N1<sup>iii</sup> atoms. On the other hand, HBs system in **2** is formed only by two interchain HBs mediated by N4–H4A...N1<sup>i</sup> and N4–H4B...N1<sup>ii</sup> atoms.

It should be also noted that different packing probably caused by different orientation of methyls leads to remarkably different

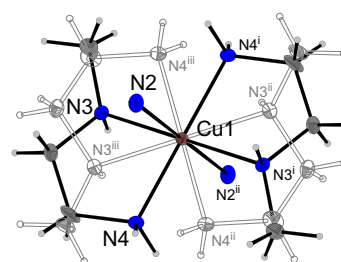


**Fig. 3.** Disordered men molecules in **2**. Symmetry operations: (i)  $-x, 1 - y, -z$ ; (ii)  $-x, 1 - y, z$ ; and (iii)  $x, y, -z$ .

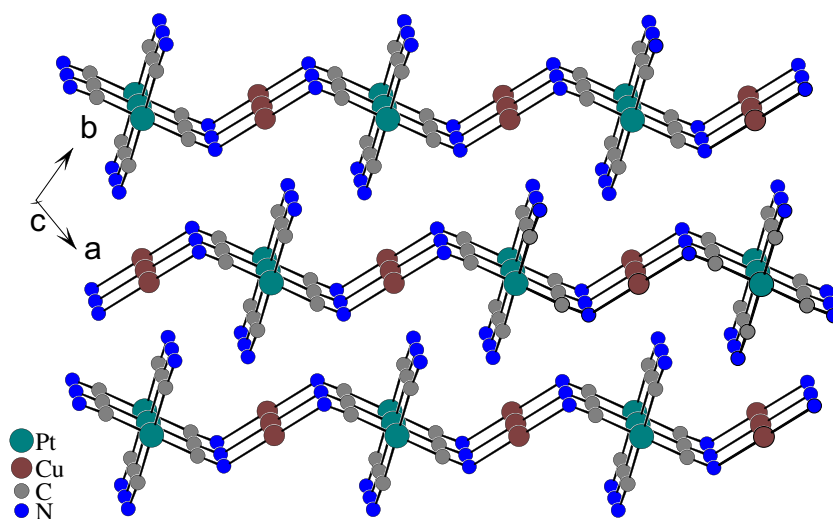


Fig. 4. Packing of the structure in **1**, showing the chains running along the [1 1 1] direction.

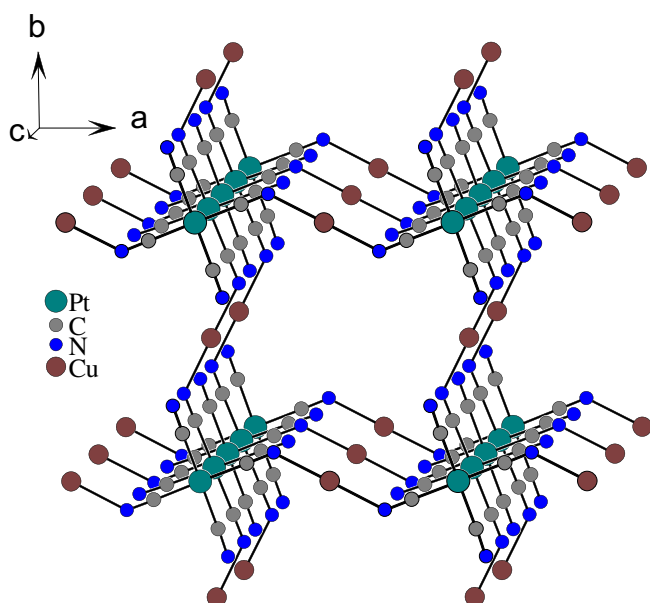


Fig. 5. Packing of the structure in **2**, showing the arrangement of chains along the *a* and *b* axes.

crystal symmetry: while **1** is a triclinic structure **2** is highly symmetrical tetragonal structure.

Parallel packing of the zigzag chains has been also observed in other 1D  $[\text{Cu}(L)_2\text{Pt}(\text{CN})_4]_n$  compounds where *L* is *en*, *dmen* and *bmen* [5,6]. If we compare the HBs systems in these compounds with that of **1**, we can summarize that bonding of only one methyl group to the N3 atoms of *men* ligands does not affect the HBs system, as one intrachain and two interchain HBs were observed in *en* complex with no methyl group, too. On the other hand, two methyl groups reduce the extent of HBs to one intrachain and one interchain HBs in the *bmen*-complex, and to only one interchain HB in *dmen*-complex. Thus, reduction of HBs system to two interchain HBs in **2** is obviously caused by different packing of the chains.

### 3.3. Spectral properties and spectral–structural correlations

The UV–vis spectra of the complexes were taken as described earlier. Broad, almost symmetric bands with maxima at 545 and

580 nm are observed in the spectra of **1** and **2**, respectively. These could be assigned to  ${}^2B_{1g} \rightarrow {}^2E_g$  transition confirming a deformed octahedral coordination geometry of the  $\text{CuN}_6$  chromophoric groups.

The IR spectra of **1** and **2** comprise bands corroborating the presence of all characteristic functional groups in the prepared complexes. Individual bands listed above in the experimental part were assigned according to the literature [25,26]. Special attention is paid to the  $\nu(\text{C}\equiv\text{N})$  stretching vibrations proving the presence of  $[\text{Pt}(\text{CN})_4]^{2-}$  units in the prepared compounds. Their positions are an important tool to distinguish between terminal and bridging character of cyanido groups. This position is observed at  $2080\text{ cm}^{-1}$  in ionic KCN as a single absorption band [26]. Upon coordination to a metal, the  $\nu(\text{C}\equiv\text{N})$  vibration shifts to higher frequencies and the range of  $\nu(\text{C}\equiv\text{N})$  for tetracyanidoplatinates(II) with terminal cyanido ligands extends from  $2120$  to  $2140\text{ cm}^{-1}$ . Because cyanido nitrogen lone pair resides in a mostly  $\text{C}\equiv\text{N}$  antibonding orbital, an increase of  $\nu(\text{C}\equiv\text{N})$  in bridging cyanides is found and for bridged tetracyanidoplatinates(II) it ranges from  $2150$  to  $2210\text{ cm}^{-1}$  [27]. Moreover, structurally different cyanido groups usually give rise to different  $\nu(\text{C}\equiv\text{N})$  vibrations and thus from the number of  $\nu(\text{C}\equiv\text{N})$  bands in the IR spectrum the number of different cyanido groups might be deduced. Hence there is a chance to predict the structural type of the corresponding tetracyanidoplatinate(II) complex. Thus, one observed  $\nu(\text{C}\equiv\text{N})$  band in the IR spectrum usually corresponds with only one kind of cyanido group in the structure of the respective, usually ionic, tetracyanidoplatinate(II) complex. However in some cases, discussed later, absorption bands of terminal and bridging cyanido groups might be overlapped and as a result only one absorption band is observed in the IR spectrum of 1D tetracyanidoplatinate(II) complex, too. Two  $\nu(\text{C}\equiv\text{N})$  absorption bands strongly indicate two identical terminal and two identical bridging cyanido groups in the 1D tetracyanidoplatinate(II) complex. Surprisingly, although there are two bridging and two terminal cyanido groups both in **1** and **2**, different number of  $\nu(\text{C}\equiv\text{N})$  absorption bands was recorded in their IR spectra (one band in **1** and two bands in **2**). Two  $\nu(\text{C}\equiv\text{N})$  vibrations have also been observed in  $[\text{Cu}(\text{men})_2\text{Ni}(\text{CN})_4]_n$  [20] and  $[\text{Cu}(\text{e-ten})_2\text{Pd}(\text{CN})_4]_n$  complexes [18] or in complexes of type  $[\text{Cu}(\text{bmen})_2\text{M}(\text{CN})_4]_n$  ( $\text{M} = \text{Ni}, \text{Pd}$  and  $\text{Pt}$ ) [28,29,6]. On the other hand, in the spectra of  $[\text{Cu}(\text{en})_2\text{M}(\text{CN})_4]_n$  ( $\text{M} = \text{Ni}, \text{Pd}$  and  $\text{Pt}$ ) [22,23,5] and  $[\text{Cu}(\text{dmen})_2\text{M}(\text{CN})_4]_n$  ( $\text{M} = \text{Ni}, \text{Pd}$  and  $\text{Pt}$ ) [28,30,5] or  $[\text{Cu}(\text{e-ten})_2\text{M}(\text{CN})_4]_n$  compounds ( $\text{M} = \text{Ni}$  and  $\text{Pt}$ ) [17] only one  $\nu(\text{C}\equiv\text{N})$  absorption band has been observed. The discrepancy in the num-

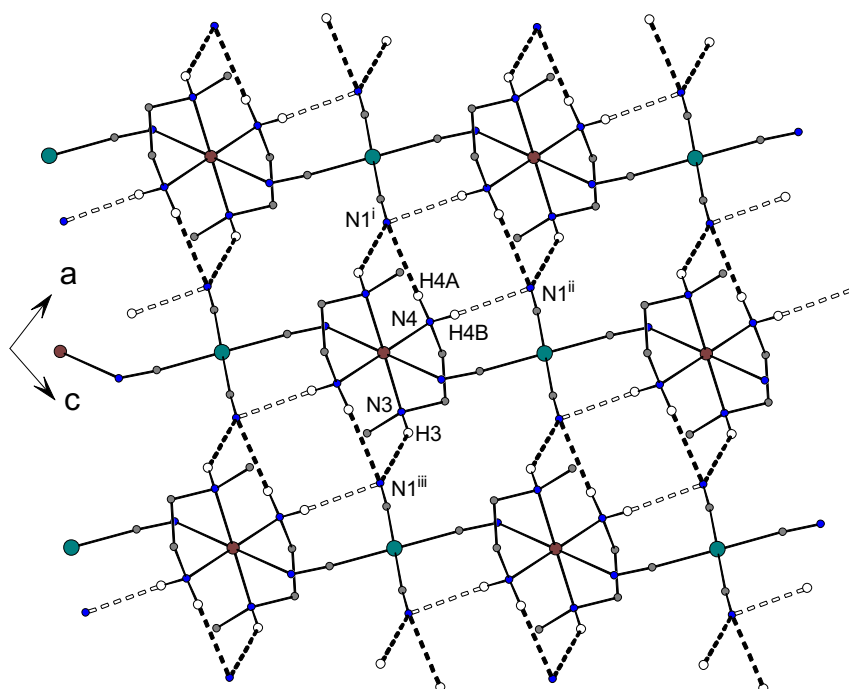


**Fig. 6.** HB system in **1**. The intrachain HBs are represented by empty dashed lines and the HBs connecting chains into sheets are represented by black dashed lines. Only hydrogen atoms of amino groups are shown because of clarity. Symmetry operations: (i)  $1 - x, -y, -2 - z$ ; (ii)  $1 + x, 1 + y, 1 + z$ ; and (iii)  $x, 1 + y, 1 + z$ .

**Table 3**  
Hydrogen bonds of **1** (Å and °).

D–H···A	$d(\text{D–H})$	$d(\text{H···A})$	$d(\text{D···A})$	$\angle(\text{D–H···A})$
N4–H4A···N1 <sup>i</sup>	0.90	2.33	3.156(4)	153.3
N4–H4B···N1 <sup>ii</sup>	0.90	2.36	3.209(3)	156.7
N3–H3···N1 <sup>iii</sup>	0.91	2.36	3.158(4)	146.6

Symmetry operations: (i)  $1 - x, -y, -2 - z$ ; (ii)  $1 + x, 1 + y, 1 + z$ ; and (iii)  $x, 1 + y, 1 + z$ .

ber of observed vibrations may be explained by the different local symmetry of  $[\text{Pt}(\text{CN})_4]^{2-}$  units in the discussed compounds. Whereas the  $\text{C}\equiv\text{N}$  bonds in **1**,  $[\text{Cu}(\text{en})_2\text{M}(\text{CN})_4]_n$ ,  $[\text{Cu}(\text{dmen})_2\text{M}(\text{CN})_4]_n$  and  $[\text{Cu}(\text{eten})_2\text{M}(\text{CN})_4]_n$  compounds differ only by 0.003 Å, corresponding difference in **2** and  $[\text{Cu}(\text{bmen})_2\text{M}(\text{CN})_4]_n$  compounds is somewhat larger. Thus, the local symmetry of  $[\text{M}(\text{CN})_4]^{2-}$  units in **1**,  $[\text{Cu}(\text{en})_2\text{M}(\text{CN})_4]_n$ ,  $[\text{Cu}(\text{dmen})_2\text{M}(\text{CN})_4]_n$  and  $[\text{Cu}(\text{eten})_2\text{M}(\text{CN})_4]_n$  compounds is  $D_{4h}$  with only one  $E_u$  IR active vibration while the local symmetry of  $[\text{M}(\text{CN})_4]^{2-}$  units in **2** and  $[\text{Cu}(\text{bmen})_2\text{M}(\text{CN})_4]_n$  compounds is  $D_{2h}$  with  $B_{2u}$  and  $B_{3u}$  IR active vibrations. The different local symmetry is also reflected by the different Cu–N(cyanido) bond lengths in **2** and  $[\text{Cu}(\text{bmen})_2\text{M}(\text{CN})_4]_n$  compounds on the one hand, and **1**,  $[\text{Cu}(\text{en})_2\text{M}(\text{CN})_4]_n$ ,  $[\text{Cu}(\text{dmen})_2\text{M}(\text{CN})_4]_n$  and  $[\text{Cu}(\text{eten})_2\text{M}(\text{CN})_4]_n$  compounds on the other hand. The corresponding Cu–N(cyanido) bond lengths in **2** and  $[\text{Cu}(\text{bmen})_2\text{M}(\text{CN})_4]_n$  compounds are less than 2.490(4) Å. However, these distances in **1**,  $[\text{Cu}(\text{en})_2\text{M}(\text{CN})_4]_n$ ,  $[\text{Cu}(\text{dmen})_2\text{M}(\text{CN})_4]_n$  and  $[\text{Cu}(\text{eten})_2\text{M}(\text{CN})_4]_n$  compounds are within the range of 2.537(1)–2.600(5) Å and, therefore, the bridging cyanido groups adopt partially ionic character and their behavior is rather close to the terminal ones. In accordance, the wavenumbers of the corresponding vibrations decrease and eventually may be overlapped by the vibrations of terminal cyanido groups. Finally, the superposition of bands might be caused by the slight increase of the position of the terminal group absorption band because of its involvement in HBs. As mentioned above, the HBs system in **1** is formed by one intrachain and two interchain HBs involving the N1 atom of the

terminal cyanido group, whereas HBs system in **2** is formed only by two interchain HBs. Because the strength of the two interchain HBs, evaluated on the base of their bonding characteristics (see bond lengths and angles in Tables 3 and 4), should be comparable we can expect larger increase of the wavenumber of the corresponding vibration in **1** and eventually it may be overlapped by the vibration of bridging cyanido groups. Therefore, only one  $\nu(\text{C}\equiv\text{N})$  absorption band in their IR spectra has been observed. According to these facts, the absorption band in the IR spectrum of **1** at  $2130\text{ cm}^{-1}$  is assigned to the vibrations of all four cyanido groups as the two Cu1–N2(cyanido) bonds are rather long (2.552(3) Å) and thus the bridging cyanido groups behave spectroscopically as terminal ones. On the other hand, as the two Cu1–N2(cyanido) bonds in **2** are shorter (2.450(3) Å), absorption bands for terminal and bridging cyanido groups are separated at 2119 and  $2129\text{ cm}^{-1}$ , respectively.

Based on the results of this and our previous work we believe that the Cu–N(cyanido) bond distance in the square-planar copper(II) tetracyanidometallates can be estimated from the number and wavenumbers of  $\nu(\text{C}\equiv\text{N})$  vibrations in the IR spectra of the corresponding complexes. There is depicted in Fig. 8 the dependence of the difference between the wavenumbers for bridging and terminal cyanido groups ( $\Delta\nu(\text{C}\equiv\text{N}) = \nu(\text{C}\equiv\text{N})_{\text{bridging}} - \nu(\text{C}\equiv\text{N})_{\text{terminal}}$ ) on the Cu–N(cyanido) bond distances for 1D  $[\text{Cu}(L)_2\text{M}(\text{CN})_4]_n$  complexes where  $L$  is *en* and its derivatives with aliphatic groups substituting amino hydrogen atoms, namely:  $L = \text{en}$  and  $M = \text{Ni, Pd}$  and  $\text{Pt}$  [22,23,5],  $L = \text{bmen}$  and  $M = \text{Ni, Pd}$  and  $\text{Pt}$  [28,29,6],  $L = \text{dmen}$  and  $M = \text{Ni, Pd}$  and  $\text{Pt}$  [28,30,5],  $L = \text{eten}$  and  $M = \text{Ni, Pd}$  and  $\text{Pt}$  [17,18],  $L = \text{men}$  and  $M = \text{Ni}$  [20], and **1** and **2**. As can be seen from this graph, with an increase of the Cu–N(cyanido) bond length, the  $\Delta\nu(\text{C}\equiv\text{N})$  is decreasing, what is also in agreement with the Scott's and Holm's work [31]. One can also see that there exists a critical Cu–N(cyanido) bond length (about 2.5 Å), above which the  $\Delta\nu(\text{C}\equiv\text{N})$  is equal to zero, what results in overlapping of the two bands and in observing only one  $\nu(\text{C}\equiv\text{N})$  absorption band.

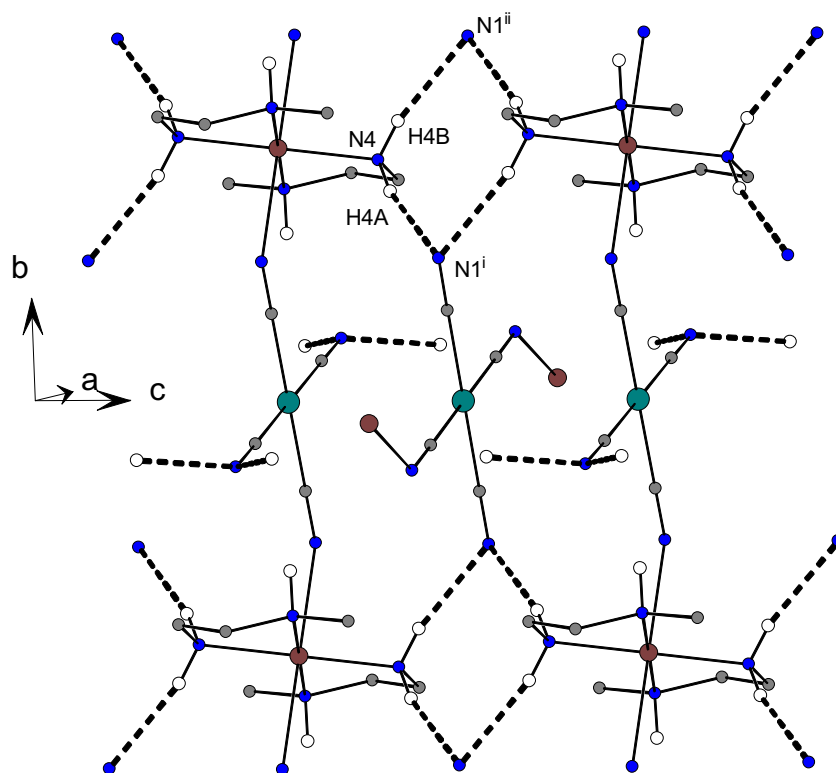


**Fig. 7.** HB system in **2**. The HBs connecting chains into sheets are represented by black dashed lines. Only hydrogen atoms of amino group are shown because of clarity. Symmetry operations: (i):  $x, -y, -1/2 + z$  and (ii)  $1 - x, y, -1/2 - z$ .

**Table 4**  
Hydrogen bonds of **2** (Å and °).

D–H...A	d(D–H)	d(H...A)	d(D...A)	<D–H...A
N4–H4A...N1 <sup>i</sup>	0.90	2.29	3.173(5)	168.6
N4–H4B...N1 <sup>ii</sup>	0.90	2.24	3.120(5)	167.4

Symmetry operations: (i)  $x, -y, -1/2 + z$  and (ii)  $1 - x, y, -1/2 - z$ .

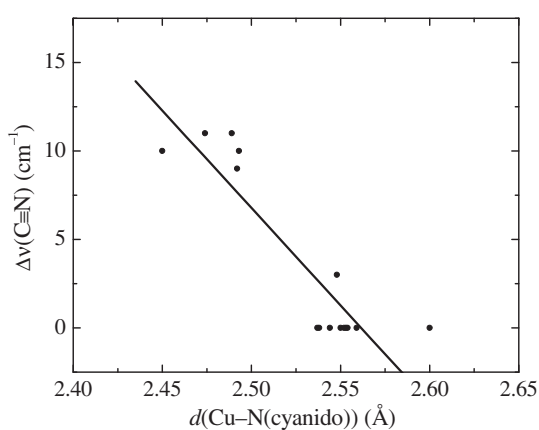


**Fig. 8.**  $\Delta\nu(\text{C}\equiv\text{N})$  dependence on  $d(\text{Cu}-\text{N}(\text{cyanido}))$  for 2,2 chain-like  $[\text{Cu}(L)_2\text{M}(\text{CN})_4]_n$  complexes ( $L = en$  and its derivatives with aliphatic groups substituting amino hydrogen atoms;  $M = \text{Ni}, \text{Pd}$  and  $\text{Pt}$ ).

### 3.4. Thermal analysis

Thermal decompositions of **1** and **2** are multistage processes similar to the thermal decompositions of other  $[\text{Cu}(L)_2\text{Pt}(\text{CN})_4]_n$  complexes which involve deamination in one or several stages fol-

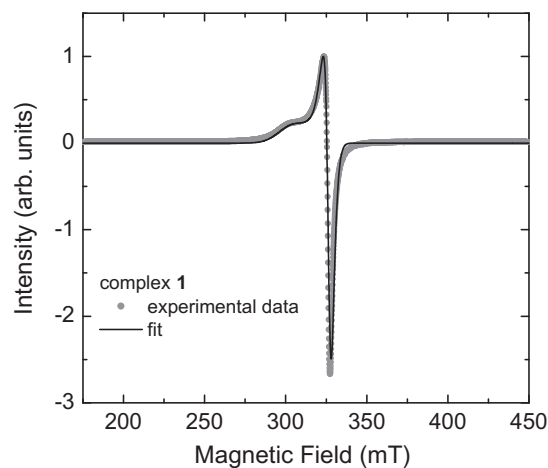


**Fig. 9.** The EPR spectrum of **1** (circles) measured at 9.4 GHz. The solid line represents a fit of a model including anisotropic  $g$ -factor ( $[g_x, g_y, g_z] = [2.058, 2.056, 2.222]$ ) and anisotropic linewidth broadening ( $[\Delta B_x, \Delta B_y, \Delta B_z] = [7.85, 3.20, 22.10]$  mT) to the experimental data.

lowed by separated decomposition of cyanido groups in one step [5,6]. Both complexes are stable up to 238 °C. In the first step, common for both complexes, in the 238–300 °C temperature range a weight loss of 13.3% and 13.7%, respectively corresponding to the release of one *men* molecule (calculated 14.5%) is observed during a slightly exothermic effect. The decomposition continuously proceeds with the next two overlapped steps which differ slightly for both complexes, thus the data for **2** are given in the brackets. In the 300–410 °C and 410–517 °C [300–454 °C and 454–648 °C] temperature ranges a weight loss of 33.3% [33.0%] is observed, which corresponds to the release of the second *men* molecule and

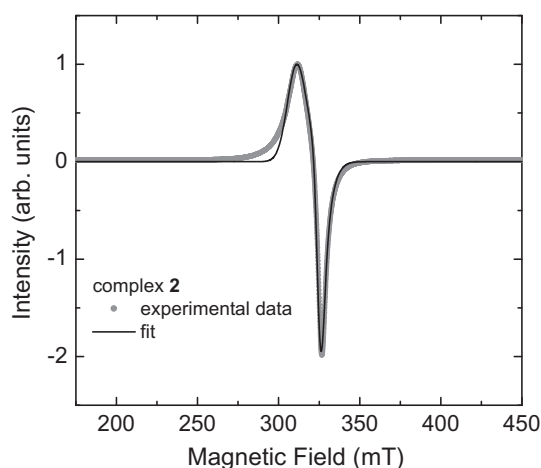


**Fig. 10.** The EPR spectrum of **2** (circles) measured at 9.4 GHz. The solid line represents a fit of a model including anisotropic  $g$ -factor ( $[g_x, g_y, g_z] = [2.065, 2.085, 2.157]$ ) and anisotropic linewidth broadening ( $[\Delta B_x, \Delta B_y, \Delta B_z] = [4.65, 20.50, 13.40]$  mT) to the experimental data.

decomposition of all four cyanido groups (calculated 34.9%). Their decomposition includes oxidation of cyanido groups to form two cyanogen molecules during the reduction of one Pt(II) to Pt atom and formation of one copper(II) oxide by the reaction with oxygen from air atmosphere. This process is accompanied by a strong exothermic effect as a consequence of the formation of cyanogen molecules as evidenced by maximum in the DTA curve at 472 °C [475 °C]. The final thermal decomposition products of both complexes are mixtures of CuO and metallic Pt (solid residue 54.5% [52.8%]; calculated 53.8%); the presence of copper(II) oxide has been confirmed by the  $\nu(\text{Cu-O})$  vibrations observed in the IR spectra at 555 and 559  $\text{cm}^{-1}$ , respectively. The most probable thermal decomposition schemes for **1** and **2** are:

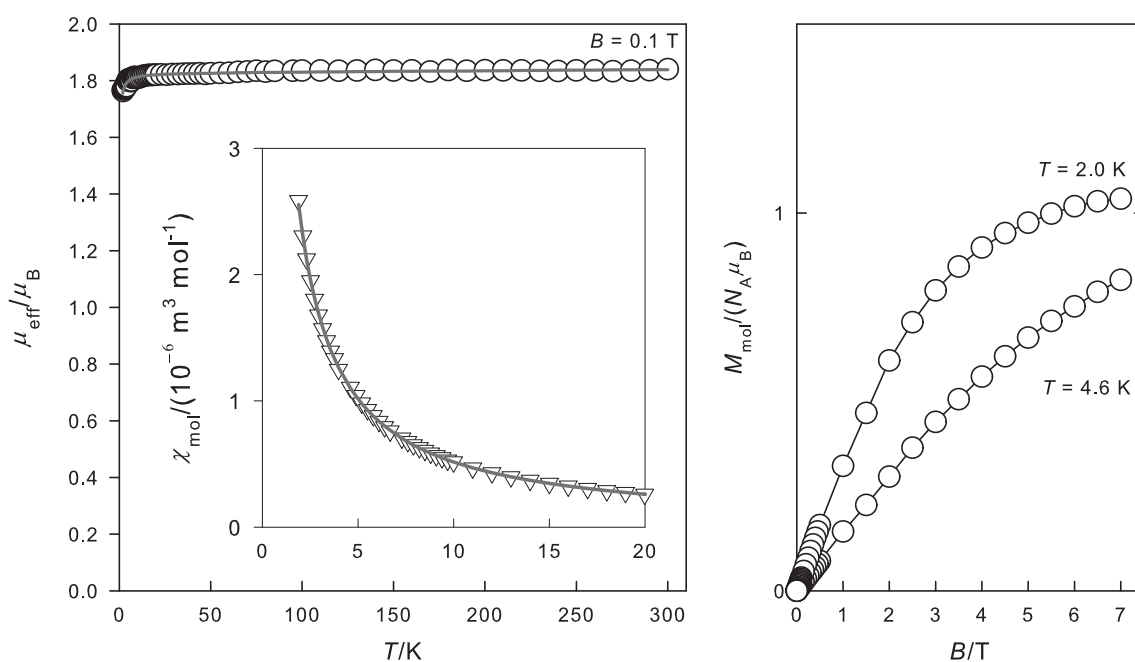
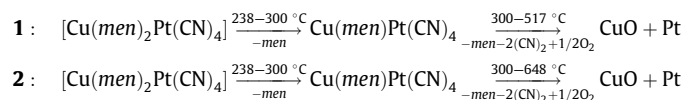


**Fig. 11.** Left: effective magnetic moment of **1** per formula unit. Inset: temperature dependence of the magnetic susceptibility. Open circles – experimental data, lines – fitted. Right: magnetization of **1** per formula unit (lines are guide for eyes).

We can conclude that the highest difference between the thermal decompositions of **1** and **2** is the temperature when cyanido groups are released, i.e. the temperature when the thermal decompositions are over. This difference might be explained by the differences in the structures of **1** and **2**.

### 3.5. Magnetic properties

The EPR spectra of **1** and **2** obtained at 2.25 K on powdered samples (Figs. 9 and 10) have been analyzed using the EPR spectra simulation package EasySpin [32]. The best agreement with the experimental data has been obtained for the following principal values of the  $g$ -tensor:  $g_x = 2.058, g_y = 2.056, g_z = 2.222$  for complex **1** and  $g_x = 2.065, g_y = 2.085, g_z = 2.157$  for complex **2**. The experimental spectra were not possible to describe using a single linewidth, therefore anisotropic broadening of the resonance line  $\Delta B = [\Delta B_x, \Delta B_y, \Delta B_z] = [7.85, 3.20, 22.10]$  mT for complex **1** and  $\Delta B = [\Delta B_x, \Delta B_y, \Delta B_z] = [4.65, 20.50, 13.40]$  mT for complex **2** was included (full width at half height). Such anisotropic linewidth broadening can reflect the low-dimensional character of the magnetic subsystem in both complexes. In addition, the unresolved hyperfine structure expected for Cu(II) atoms due to the existence of exchange couplings between magnetic centers [33] results in anisotropic broadening of the resonance line. The anisotropic  $g$ -factors are consistent with the axial type of anisotropy due to the Jahn–Teller effect typical for spin  $S = 1/2$  Cu(II) atoms including the influence of a weak rhombic distortion of the coordination octahedron. The results confirm that the electronic ground state of the Cu(II) ion is described by a wave function of  $d_{z^2}$  symmetry and the exchange paths will propagate along the directions determined by the lobes of the  $d_{x^2-y^2}$  orbital. The difference in the linewidth anisotropy for complex **1** and **2** can be explained by different strength and orientation of exchange paths due to the differences in HB network between the chains.

The magnetic susceptibility taken at  $B = 0.1$  T has been converted to the effective magnetic moment, as displayed in Figs. 11 and 12. Its room temperature value amounts to  $\mu_{\text{eff}} = 1.84 \mu_B$  in both complexes and this value stays almost constant down to 7 K for **1** and 22 K for **2** when it turns down. Such a behavior is typical

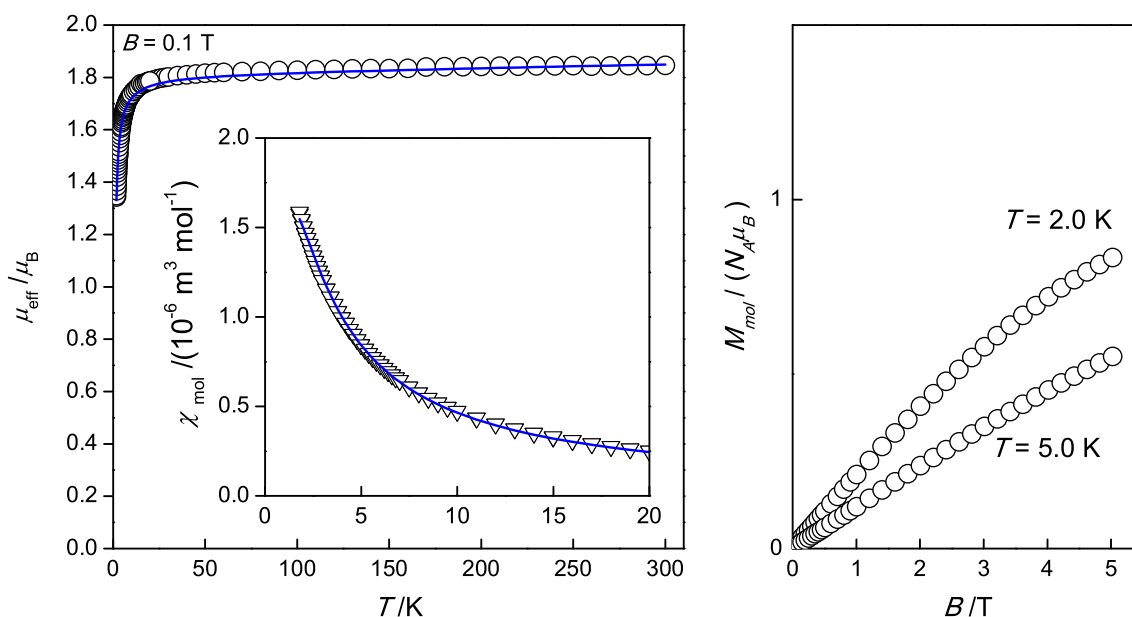


**Fig. 12.** Left: effective magnetic moment of **2** per formula unit. Inset: temperature dependence of the magnetic susceptibility. Open circles – experimental data, lines – fitted. Right: magnetization of **2** per formula unit (lines are guide for eyes).

for a regular  $s = 1/2$  chain exhibiting antiferromagnetic exchange. In order to fit the susceptibility data several methods have been proposed [34–39] of which the Bonner–Fischer formula belongs to the most popular [40,41]. The original formula has been rescaled by Kahn [11] in order to accommodate the  $\hat{H}_{A,A+1} = -J(\hat{S}_A \cdot \hat{S}_{A+1})\hbar^{-2}$  notation for the exchange coupling constant. The fitting procedure gave  $J/\hbar c = -0.17 \text{ cm}^{-1}$ ,  $g = 2.11$  and the uncompensated temperature-independent magnetism of  $\chi_{\text{TIM}} = +0.23 \times 10^{-9} \text{ m}^3 \text{ mol}^{-1}$  (discrepancy factor  $R(\chi) = 0.007$ ) for **1**, while for **2** yielded  $J/\hbar c = -1.3 \text{ cm}^{-1}$ ,  $g = 2.09$  and  $\chi_{\text{TIM}} = +0.73 \times 10^{-9} \text{ m}^3 \text{ mol}^{-1}$ . Such a small value of the coupling constant causes that the expected maximum on the susceptibility curve lies below the temperature limit of set-up (1.8 K). Since the HBs create shorter exchange paths (see Figs. 6 and 7) between the Cu(II) centers in the direction of magnetic orbitals in complex **2**, the coupling constant is stronger than in complex **1**. A weak antiferromagnetic exchange coupling is similar to that of other compounds from our previous studies [5,6].

#### 4. Conclusion

Violet (**1**) and blue crystalline (**2**) polymorphous modifications of  $[\text{Cu}(\text{men})_2\text{Pt}(\text{CN})_4]_n$  complex, suitable for X-ray structural analysis have been prepared by hydrothermal syntheses. Both modifications are formed by very similar 2,2-*TT* zigzag chains in which  $[\text{Cu}(\text{men})_2]^{2+}$  moieties are connected by  $[\text{Pt}(\text{CN})_4]^{2-}$  units. Cu(II) atoms in both modifications are coordinated by four N atoms of two bidentate *men* ligands in the equatorial plane whereas the axial positions are occupied by two N atoms of bridging cyanido groups at substantially longer distances due to Jahn–Teller effect. The structures differ in bond parameters, in arrangement of methyl groups of *men* ligands, in packing of the chains and in hydrogen bonds system in **1** and **2**. Different bond lengths within  $[\text{Pt}(\text{CN})_4]^{2-}$  units in **1** and **2** induce a different local symmetry of these units and this manifests itself by different number of  $\nu(\text{C}\equiv\text{N})$  vibrations in the IR spectra. Wavenumbers of these vibrations are correlated with Cu–N(cyanido) bond length. Broad, almost symmetric bands observed in the electronic spectra of **1** and **2**, which could be assigned to  ${}^2B_{1g} \rightarrow {}^2E_g$  transition confirm a deformed octahedral coordination of the  $\text{CuN}_6$  chromophoric groups. Complexes **1** and

**2** are stable up to 238 °C when their two-stage thermal decompositions start towards a mixture of CuO and metallic Pt as the most probable final thermal decomposition products. The temperature dependence of the inverse susceptibility suggests the presence of a weak antiferromagnetic exchange coupling between Cu(II) atoms in **1** and **2**.

#### Acknowledgments

This work was supported by the grants of the Slovak Grant Agency VEGA 1/0079/08, 1/0213/08, and 1/0078/09, by Slovak Research and Development Agency under the Contract Nos. APVV-VVCE-0058-07, APVV-VVCE-0004-07 and APVV-0006-07, by the Institutional Research Plan No. AVOZ10100521 of the Institute of Physics and the Project Praemium Academiae of the Academy of Sciences of the Czech Republic. M.V. thanks DAAD for financial support and hospitality of Martin–Luther–University. E.Č., S.A.Z. and M.O. would like to acknowledge the support by the Deutsche Forschungsgemeinschaft and EuroMagNET (EU Contract No. 228043). The authors are very grateful to Dr. Vladimír Zelenák from P.J. Šafárik University in Košice for the thermal analysis measurements.

#### Appendix A. Supplementary data

CCDC 784112 and 784113 contain the supplementary crystallographic data for complexes **1** and **2**. These data can be obtained free of charge via <http://www.ccdc.cam.ac.uk/conts/retrieving.html>, or from the Cambridge Crystallographic Data Centre, 12 Union Road, Cambridge CB2 1EZ, UK; fax: (+44) 1223-336-033; or e-mail: deposit@ccdc.cam.ac.uk.

#### References

- [1] M. Pilkington, S. Decurtins, in: A. McCleverty, T.J. Meyer (Eds.), *Comprehensive Coordination Chemistry II*, vol. 7, Elsevier, Amsterdam, 2004.
- [2] K.R. Dunbar, R.A. Heintz, *Prog. Inorg. Chem.* 45 (1997) 283.
- [3] J. Černák, M. Orendáč, I. Potočník, J. Chomič, A. Orendáčová, J. Skoršepa, A. Feher, *Coord. Chem. Rev.* 224 (2002) 51.
- [4] H. Vahrenkamp, A. Geib, G.N. Richardson, *J. Chem. Soc., Dalton Trans.* (1997) 3643.

- [5] I. Potočňák, M. Vavra, E. Čižmár, K. Tibenská, A. Orendáčová, D. Steinborn, C. Wagner, M. Dušek, K. Fejfarová, H. Schmidt, T. Müller, M. Orendáč, A. Feher, *J. Solid State Chem.* 179 (2006) 1965.
- [6] I. Potočňák, M. Vavra, E. Čižmár, M. Kajňáková, A. Radváková, D. Steinborn, S.A. Zvyagin, J. Wosnitzer, A. Feher, *J. Solid State Chem.* 182 (2009) 196.
- [7] M. Vavra, I. Potočňák, D. Steinborn, C. Wagner, *Acta Cryst. E* 62 (2006) m1895.
- [8] I. Potočňák, M. Vavra, E. Čižmár, M. Dušek, T. Müller, D. Steinborn, *Inorg. Chim. Acta* 362 (2009) 4152.
- [9] I. Potočňák, M. Vavra, *J. Chem. Cryst.* 40 (2010) 993.
- [10] G.B. Kaufmann, *Inorg. Synth.* 9 (1967) 182.
- [11] O. Kahn, *Molecular Magnetism*, VCH, New York, 1993.
- [12] Oxford Diffraction, *Crysalis CCD and Crysalis RED*, Oxford Diffraction Ltd., Oxford, UK, 2004.
- [13] G.M. Sheldrick, *SHELXS97 and SHELXL97*, University of Göttingen, Göttingen, Germany, 1997.
- [14] V. Petříček, M. Dušek, L. Palatinus, *JANA2006. The Crystallographic Computing System*, Institute of Physics, Praha, Czech Republic.
- [15] K. Brandenburg, *DIAMOND, Release 2.1e, Crystal Impact GbR*, Bonn, Germany, 2000.
- [16] R.C. Clark, J.S. Reid, *Acta Cryst. A* 51 (1995) 887.
- [17] T. Akitsu, Y. Einaga, *Inorg. Chim. Acta* 360 (2007) 497.
- [18] T. Akitsu, Y. Endo, *Acta Cryst. E* 65 (2009) m406.
- [19] A. Karadag, A. Senocak, I. Önal, Y. Yerli, E. Sahin, A. Cemil Basaran, *Inorg. Chim. Acta* 362 (2009) 2299.
- [20] J. Kuchár, J. Černák, Z. Žák, W. Massa, *Progress in Coordination and Bioinorganic Chemistry*, STU Press, Bratislava, 2003, p. 127.
- [21] A.B.P. Lever, *Inorganic Electronic Spectroscopy*, Elsevier, Amsterdam, 1984.
- [22] K. Seitz, S. Peschel, D. Babel, Z. Anorg. Allg. Chem. 627 (2001) 929.
- [23] J. Černák, J. Skoršepa, K.A. Abboud, M.W. Meisel, M. Orendáč, A. Orendáčová, A. Feher, *Inorg. Chim. Acta* 326 (2001) 3.
- [24] T. Akitsu, Y. Einaga, *Inorg. Chem.* 45 (2006) 9826.
- [25] Z. Gabelica, *Spectrochim. Acta* 32A (2) (1976) 337.
- [26] K. Nakamoto, *Infrared and Raman Spectra of Inorganic and Coordination Compounds, Part B: Applications in Coordination, Organometallic and Bioinorganic Chemistry*, Wiley, New York, 1997.
- [27] A.M. Golub, H. Köhler, V.V. Skopenko, *Chemistry of Pseudohalides*, Elsevier, Amsterdam, 1986.
- [28] J. Kuchár, J. Černák, Z. Mayerová, P. Kubáček, Z. Žák, *Solid State Phenom.* 90 (2003) 323.
- [29] J. Hanco, M. Orendáč, J. Kuchár, Z. Žák, J. Černák, A. Orendáčová, A. Feher, *Solid State Commun.* 142 (2007) 128.
- [30] J. Kuchár, J. Černák, K.A. Abboud, *Acta Cryst. C* 60 (2004) m492.
- [31] M.J. Scott, R.H. Holm, *J. Am. Chem. Soc.* 116 (1994) 11357.
- [32] S. Stoll, A. Schweiger, *J. Magn. Reson.* 178 (2006) 42.
- [33] D. Gatteschi, A. Bencini, *Electron Paramagnetic Resonance of Exchange Coupled Systems*, Springer, Berlin, 1990.
- [34] G.A. Baker Jr., G.S. Rushbrooke, H.E. Gilbert, *Phys. Rev.* 135 (1964) A1272.
- [35] A. Meyer, A. Gleizes, J.J. Girend, M. Verdaguer, O. Kahn, *Inorg. Chem.* 21 (1982) 1729.
- [36] W. Hiller, J. Strähle, A. Datz, M. Hanach, W.E. Hatfield, *J. Am. Chem. Soc.* 106 (1984) 329.
- [37] C.H. Weng, *PhD. Thesis*, Carnegie-Mellon University, Pittsburgh, PA, 1968.
- [38] R. Feyerherm, S. Abens, D. Günther, T. Ishida, M. Meissner, M. Meschke, T. Nogami, M. Steiner, *J. Phys. Condens. Matter* 12 (2000) 8495.
- [39] D.C. Johnston, R.K. Kremer, M. Troyer, W. Wang, A. Klümper, S.L. Budko, A.F. Panchula, P.C. Canfield, *Phys. Rev. B* 61 (2000) 9558.
- [40] J.C. Bonner, M.E. Fischer, *Phys. Rev.* 135 (1964) A640.
- [41] W.E. Estes, D.P. Gavel, W.E. Hatfield, D.J. Hodgson, *Inorg. Chem.* 17 (1978) 1415.